

Modification of the Traditional Half Schlumberger Arrays and its Efficiency for Subsurface Exploration

Diya'ulhaq Abdullahi^{1*}, Nura Muhammad Nagoda², Emmanuel Jaiyeoba³, Salisu Musa¹, Abubakar Muhammad⁴, Muhammad Ridwan Mahamood⁴, Aliyu Usman Musa⁵, Muhammad Sanusi Lawan⁶ & Abdulazeez Shehu⁷

¹Department of Physics, Air Force Institute of Technology, Kaduna, Nigeria.

²Department of Physical Science, Kano State Polytechnic

³Department of Physics, Kaduna State University, Kaduna, Nigeria.

⁴Department of Applied Geophysics, Federal University Birnin Kebbi.

⁵Department of Physical Science, Niger State Polytechnic, Zungeru.

⁶Department of Physics, Bayero University, Kano.

⁷Department of Physics, Federal University of Technology Babura, Jigawa State.

*Corresponding author: Diya'ulhaq Abdullahi, Department of Physics, Air Force Institute of Technology, Kaduna, Nigeria.

Submitted: 01 February 2024 Accepted: 07 February 2024 Published: 14 February 2024

 <https://doi.org/10.63620/MKJAEES.2024.1025>

Citation: Abdullahi, D., Nagoda, N. M., Jaiyeoba, E., Musa, S., Muhammad, A., Mahamood, M. R., Musa, A. U., Lawan, M. S., & Shehu, A. (2024). Modification of the Traditional Half Schlumberger Arrays and its Efficiency for Subsurface Exploration. *J of Agri Earth & Environmental Sciences*, 3(1), 01-12.

Abstract

The geophysical investigation of the earth's subsurface is a vital step in engineering and environmental surveys. Application of the basic methods of geophysics to detect and study subsurface anomalies for engineering and environmental problems. This study modified the existing Half Schlumberger arrays after evaluating the efficiency of the existing Half Schlumberger array. The Modified Half Schlumberger (SMH) relatively produces a better result for a deeper geophysical investigation where there is a limited space than the existing Half Schlumberger (SH). The results of the investigated nine (9) VES stations were presented in tables and graphs, which shows that the two arrays are nearly the same (about 94% in similarity). The SMH array shows an interesting result. It was noted that the SMH probes were deeper than the usual SF arrays with an average extension of about 2.4 m depth in terms of overburden thickness. In addition, the two arrays produce identical curve types, subsurface parameters, and soil depth section sequences across all the VES stations. The identical results confirmed the efficiency and reliability of the SMH array. Consequently, SMH can be adopted as a practicable alternative array to the traditional SH and the conventional Full Schlumberger (SF) array for any geophysical survey, where the usual SF array is applicable, most especially when deeper subsurface information is required and the available space is highly limited.

Keywords: Half Schlumberger, Modified Half Schlumberger, Efficiency, Alternative Array, Overburden Thickness.

Introduction

The investigation of the earth's subsurface to a large extent; can only be done through drilling before the coming of geophysics. The drilling process is time-consuming, highly expensive, tedious, and destructive [1, 2, 3]. However, geophysics investigation by drilling appears more certain and accurate, but it is highly limited because it can only provide subsurface information at a discrete location, and it is highly restricted to a certain terrain [4, 5, 6, 1]. Studies have shown that all geophysics explorations and theoretical analysis of acquired data are less effective when compared to physical drilling [2, 3]. Therefore, the involvement of geophysics in subsurface exploration such as environmental engineering has become a prominent and promising approach [7, 8, 9, 10]. Geophysical methods are implemented in a wide range of applications ranging from magnetic, gravity, seismic,

electrical resistivity, electromagnetic, induced polarization, radioactive, and so on [4]. However, electrical resistivity surveys remain one of the most efficient and suitable methods for groundwater exploration,

especially for depth information [11, 12, 13]. However, many configurations of electrodes have been designed for electrical resistivity surveys (Vertical electrical sounding), which are occasionally employed in specialized surveys such as mineral and groundwater exploration [7, 14, 15, 16, 17, 18]. In Vertical electrical sounding, different kinds of arrays can be used to exploit the information of the earth's subsurface such as lithology, hydro-geological, and stratigraphic sequence characteristics, and the subsurface strata can be obtained through the help of electrical resistivity survey techniques [4]. The electrical resistivity

ty technique has been widely used and accepted in prospecting for foundation studies, groundwater dam site location, pollution plumes, mineral exploration, and road failures [17, 19]. However, the electrical method is usually challenged by limited space for the spreading of cables, which could lead to incomplete investigation, wrong judgment, and wrong recommendations due to incomplete information obtained from the little spreading [5, 20].

However, electrical resistivity which appears to be the most common geophysics technique currently in use; involves the injecting of an electrical current into the ground through steel electrodes in an attempt to measure the electrical properties of the subsurface of the earth [7, 21, 22, 23]. The Schlumberger array configuration of Vertical Electrical Sounding (VES) is one of the most commonly used techniques in the electrical resistivity survey due to its capacity to probe deeper when compared to the Wenner array [24, 25]. According to remarkable studies show that the Schlumberger and Wenner methods are not applicable where there is urban development as well as congested village community areas, because of limited space for lateral spread of the electrodes [26, 27]. As a result, care should be taken while giving suitable sites. In both techniques, it is necessary to operate on a dry surface for effective penetration of the current and if the ground is wet or if sufficient moisture is present in the ground, likely that the current will not penetrate the ground [28, 29, 30].

Schlumberger has been considered one of the most effective techniques for deeper information, especially for the delineation of groundwater potential over time. This is because it provides a better vertical resolution, it takes less time to be achieved, and it requires less manpower (only three people can conveniently carry out the Schlumberger array technique) [31, 32, 20]. Despite the advantages of this Schlumberger array, its applications are limited in a congested and built-up environment where deeper subsurface information is required [5, 33]. This implies that; Schlumberger's investigation becomes extremely difficult in such congested terrain. Due to this inadequate space, the depth of investigation may be reduced and geo-electrical results become inconclusive, which may result in incomplete recommendations [20]. In such a congested and built environment, a modified array which is known as Half Schlumberger was de-

veloped to tackle the problem of inadequate space, since one electrode can be kept constant or fixed perpendicularly (900) very far away, while moving the second current electrode. With this, it was discovered that the Half Schlumberger array is more convenient, fast, easy, and requires less manpower compared to the Full Schlumberger, as only two persons can conveniently carry out the survey. The effectiveness and efficiency of the half Schlumberger array have been fully confirmed and affirmed [5, 33, 20]. This research work attempts to improve on the Half Schlumberger by modifying the usual Half Schlumberger arrays where the current electrode B is kept at an infinite distance (that is; the current electrode B is placed at a position where B is three times the distance $AB/2$ or $L/2$). The modification developed by work is targeted at the extension of the constant current electrode B from its usual distance $B = 3(AB/2)$ to a position where $B = 4(AB/2)$. That is, the current electrode B would now be placed at a position four times the traditional Full Schlumberger of $AB/2$.

Materials and Methods

The geo-electrical resistivity field data were acquired with the help of the earth resistivity meter commonly known as the Ohm Ω resistivity Meter. the survey makes use of several other instruments for data collection, which include; a field hammer, magnetic compass, cutlass, electrodes, measuring tape, cables and reels, as well as a Global Positioning System (GPS) Navigator, to register the geographic coordinates of the digitized VES points. The Half Schlumberger array method follows the same procedure as an electrical resistivity technique which involves the spreading of current electrodes (A & B), while the potential electrode (C & D) remains fixed (Fig 1) The objective of VES is to register the changes in resistivity values with depth and to compare it with the available geological data to infer the depths and resistivity values of the layers present [26]. The resistivity of the strata is determined by passing an electric current between two electrodes on the surface. The spacing between the electrodes was increased to obtain more subsurface information in the deeper sections, since, the depth of penetration increases the distance between electrodes increases also. In a Schlumberger array, the potential electrodes (C and D) are determined by injecting current into the ground through two steel electrodes (A and B) [4]. According to Ohm's law:

$$\Delta V = IR \quad \therefore \quad R = \frac{\Delta V}{I} \quad (1)$$

Theoretical Background of Current Flow in the Ground

Since the resistivity of a material can be defined as the resistance in Ohms between the opposite faces of a unit cube of the material (Kearey, et al., 2002), a conducting cylinder of resistance (δR), length (δL) and cross-sectional area (δA) (Fig. 2) and the resistivity ρ can be expressed by;

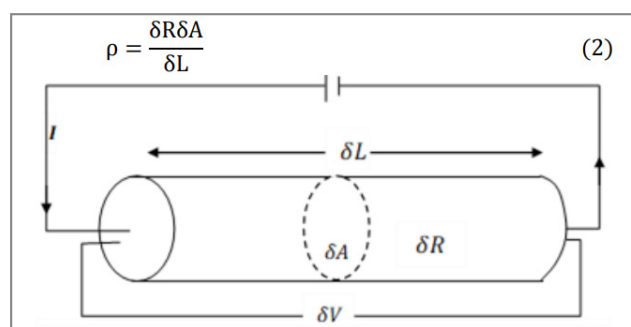


Figure 1: The Parameters used in Defining Resistivity

In an element of homogeneous material, the current (I) passed through the cylinder causes the potential drop ($-\delta V$) between the ends of the element [7, 34]. Ohm's law relates the current, potential difference and resistance such that:

$$-\delta V = \delta RI \quad (3)$$

So that:

$$\frac{\delta V}{\delta L} = -\frac{\rho I}{\delta A} \quad (4)$$

$\frac{\delta V}{\delta L}$ represents the potential gradient through the element, measures in volt m^{-1} and J the current density in Am^{-2} . Now, consider a single current electrode on the surface of a medium of uniform resistivity ρ (Fig. 2). The circuit is completed, when a current sink at a large distance from the electrode [7]. The current flows radially away from the electrode; so that the current is uniformly distributed over hemispherical shells centred on the source [35, 4]. At a distance (r), the electrode of the shell has a surface area of $2\pi r^2$, so that the current density, J is given by

$$J = \frac{I}{2\pi r^2} \quad (5)$$

So, from equations (1), the potential gradient associated with this current density is defined as:

$$\frac{\partial V}{\partial r} = -\frac{\rho I}{2\pi r^2} \quad (6)$$

The potential (V_r) at distance r is then obtained by integration;

$$V_r = \int \partial V = -\int \frac{\rho I \partial r}{2\pi r^2} = \frac{\rho I}{2\pi r} \quad (7)$$

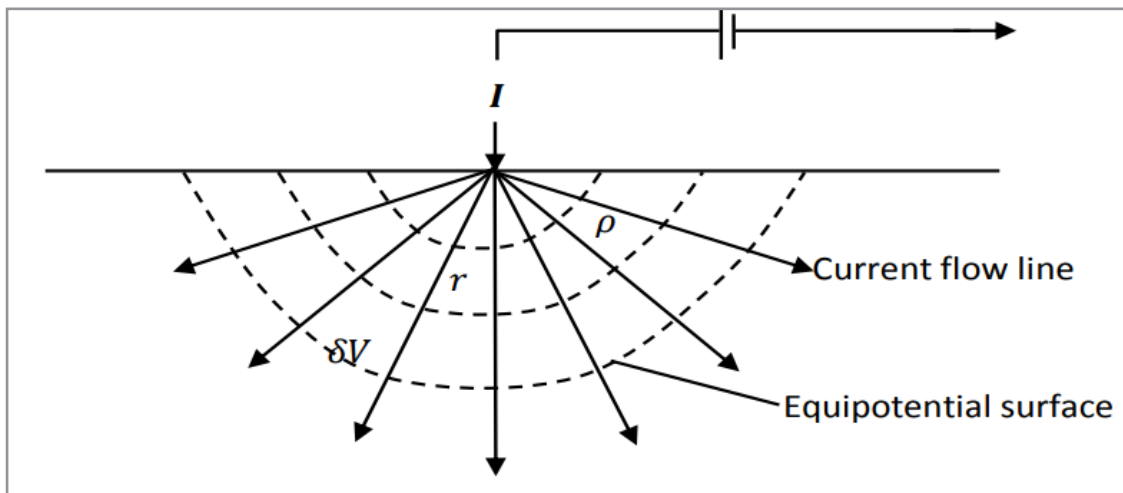


Figure 2: Current flow from a single surface electrode.

Electrode Configuration

The general formula for the resistivity measured by a four electrodes method is simpler for some special geometry of the current and potential electrodes [36]. When the current sink is at a finite distance from the source (Fig 3). The potential (V_c) at an internal electrode C is the sum of the potential contributions (V_A) and (V_B) from the current source at A; and the sink at B.

$$V_C = V_A + V_B \quad (8)$$

From (1)

$$V_C = \frac{\rho I}{2\pi} \left[\frac{1}{r_A} - \frac{1}{r_B} \right] \quad (9)$$

Similarly,

$$V_D = \frac{\rho I}{2\pi} \left[\frac{1}{R_A} - \frac{1}{R_B} \right] \quad (10)$$

Absolute potentials are difficult to monitor, so the potential difference (ΔV) between electrodes C and D is measured

$$\Delta V = V_C - V_D = \frac{\rho I}{2\pi} \left[\left(\frac{1}{r_A} - \frac{1}{r_B} \right) - \left(\frac{1}{R_A} - \frac{1}{R_B} \right) \right] \quad (11)$$

Thus, the apparent resistivity (ρ_a) can be estimated as:

$$\rho_a = \rho_a = \frac{2\pi \Delta V}{I \left[\left(\frac{1}{r_A} - \frac{1}{r_B} \right) - \left(\frac{1}{R_A} - \frac{1}{R_B} \right) \right]} = KR \quad (12)$$

Where k is the geometric factor (K-factor) and its values depend on the arrangement and configuration of the four (4) electrodes as shown in Fig 1, (Telford et al., 1990; Loke, (1990), John, 2003). According to Fig 1,

$$\left(\text{if, } AC = BD = \left(\frac{L-a}{2} \right) \text{ and } CB = AD = \left(\frac{L+a}{2} \right) \right).$$

So that, the geometry factor for the Conventional Schlumberger array, becomes:

$$K = 2\pi \frac{V}{I} \left[\left(\frac{2}{L-a} - \frac{2}{L+a} \right) - \left(\frac{2}{L+a} - \frac{2}{L-a} \right) \right]^{-1} \quad (13)$$

Equation (13), can be expressed further, so that:

$$K_F = \frac{\pi}{4} \left[\frac{L^2 - a^2}{a} \right] \quad (14)$$

Consequently, by substituting equations (14) in (12), the equation (12) becomes

$$\rho_a = RK_F = \frac{\pi \Delta V}{4I} \left[\frac{L^2 - a^2}{a} \right] \quad (15)$$

Where ρ_a = apparent resistivity measures in Ohm-meter (Ωm), K_F = geometry factor for Full Schlumberger, while parameters “L” and “a” are well illustrated and defined in Fig 1. Thus, equations

(4) and (5) can be used to calculate the geometric factor and apparent resistivity for conventional (Full) Schlumberger array configuration.

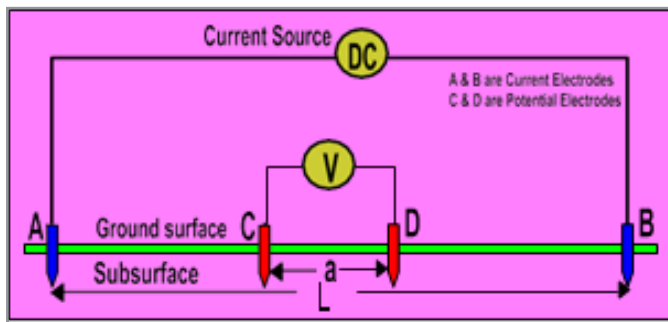


Figure 3: The Schlumberger Configuration Array Measurements

Schlumberger Array Configurations

Selection of site is extremely important in all sounding investigations, especially with the Schlumberger array due to its sensitivity to environmental conditions [14, 37, 38]. The basic focus of this research is to consider the existing Half Schlumberger technique and modifies it to produce better results. To do this, we need to review our understanding of the Schlumberger method and its applications. Schlumberger array apparent resistivities are normally estimated from the approximate equation (14). The

choice of the array and its dimension largely depends upon the target; its size, depth and resistivity contrast with its surroundings. For this present study, two different Schlumberger array configurations were exploited. Schlumberger array can provide accurate depth, thickness, electrical resistivity, depth to the water table, and bedrock estimations of the subsurface layers. It can be used to estimate geological formations as well as detection and location of contaminant plumes [7]. However, Schlumberger data are ambiguous, because many different “models” can produce the same data. Though; the Schlumberger survey is slow because electrodes must be removed and driven into the ground between measurements, the Half Schlumberger technique is very fast and easy [39]. However, the data acquired by the Schlumberger survey are usually influenced by near-surface conductive layers because the current always travels most easily along highly conductive layers and if the surface is highly conductive, it may not be possible to collect data below the top layer [29, 26]. The Schlumberger survey is one of the most common electrical techniques in the last decade for the following reasons:

1. Near-surface effect, lateral in-homogeneities affect are less with Schlumberger measurements
2. It has an excellent vertical resolution and good depth sensitivity compared to Wenner profiling
3. Schlumberger interpretation techniques are more fully developed and diversified compared to Wenner.
4. The Schlumberger array provides a reduced signal to noise ratio, and may offer an improved imaging resolution
5. It may pick up noise than the normal array when assessing the data quality using reciprocal measurements.
6. Schlumberger requires fewer manpower and electrodes, to be moved for each sounding compared to Wenner.

Calculation of Geometry Factor (K-Factor)

The common guideline adopted in a Schlumberger survey is that the CD should not exceed 20% AB/2 was adopted [4, 7]. The process yields a rapidly decreasing potential difference across space, CD, that ultimately exceeds the measuring capabilities of the instrument [7, 21, 40]. Hence, at this point, a new value for CD is established, typically 3-4 times larger than the proceeding values, and the survey continues until the last two or three AB/2 is duplicated with the new CD value. To illustrate this, we started the survey with CD = 0.3 m, increase to 1.0 m, and finally, 5.0 m, while the AB/2 starts from 1.0 m, 1.5m, and ends at 70 m. The K-factor obtained from equation (14) and presented in table 1

Table 1: Geometry Factors Computed from Full Schlumberger Array

S/N	$\left(\frac{AB}{2} \right) = \left(\frac{L}{2} \right) \text{ (m)}$	$\left(\frac{CD}{2} \right) = \left(\frac{L}{2} \right) \text{ (m)}$	$K_F = \frac{\pi}{4} \left[\frac{L^2 - a^2}{a} \right]$
1	1.0	0.3	4.76
2	1.5	0.3	11.31
3	2.0	0.3	20.47
4	3.0	0.3	46.65
5	4.5	0.3	105.56
6	7.0	0.3	256.1
8	10.0	1.0	155.51
9	15.0	1.0	351.86

10	20.0	1.0	626.75
11	30.0	1.0	1412.15
12	45.0	1.0	3179.3
13	45.0	5.0	628.32
14	70.0	5.0	1531.53

Method 1: Half Schlumberger Configuration

The usual Half Schlumberger followed the same principle of full usual conventional Schlumberger, except that, one of the current electrodes, (B) is placed at a distance, far away from the measurement area (Fig 4). To satisfy the condition for half Schlumberger array, the current electrode B must always be at a distance, $L = 3(AB/2)$, which is equivalent to 210 m for this research, since the maximum spread for this research of $AB/2 = 70$ m [32, 20]. However, since only one current electrode is moving, this method saves a lot of time, while avoiding conflicts in a congested and complex terrain. The resistivity distribution with depth, which results in deeper layers, reflects the change of apparent resistivity [41, 42, 43]. That is, whenever, deep subsurface information is required, the distance $AB/2$ increases; and the current penetrates deeper than the previous one [32, 20]. The

geometric factor of the Half Schlumberger array has been evaluated to be twice that of the usual full Schlumberger array. So that the geometric factor for Half Schlumberger can be expressed as:

$$K_H = 2K_F = 2 \cdot \frac{\pi}{4} \left[\frac{L^2 - a^2}{a} \right] = \pi \left[\frac{L^2 - a^2}{2a} \right] \quad (16)$$

So that:

$$\rho_a = 2RK_F \quad (17)$$

Where K_F and K_H = geometry factors for Full Schlumberger and Half Schlumberger respectively.

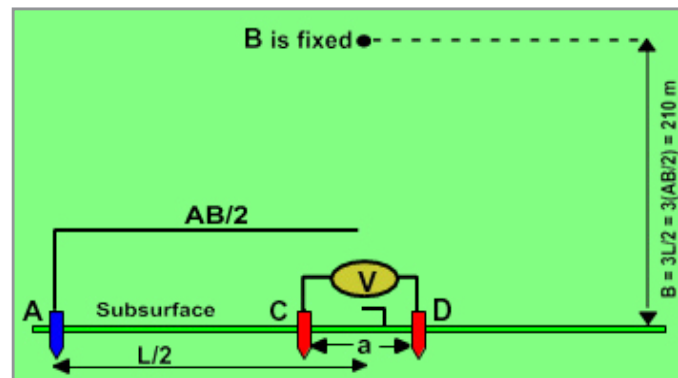


Figure 4: Configuration of the Half Schlumberger Arrays (B at $3L/2$)

Method 2: Modified Half Schlumberger Configuration

Modified Half Schlumberger (SMH) is the main focus and the gap bridged by this work. Note that the method adopted by SMH is the same as the principle of the usual traditional SF and the normal SH, except that, this time, the current electrode (B) was placed at a position that is far away, when compared to the known half Schlumberger (Fig 5). That is, the major difference between the half Schlumberger and the modified half Schlumberger is the position of current electrode B. In a modified half Schlumberger array, we placed the current electrode, B at a distance $B = 2L = 2(AB) = 2 \times 140 = 280$ m (Fig 5), since $AB/2$ for this survey is 70 m. The geometric factor of the Modified Half Schlumberger arrays was derived from the existing Full and Half Schlumberger according to equations (16) and (17). We can now evaluate the geometric factor for the Modified Half Schlumberger (KMH) arrays from equations (15), (16), and (17) as follow:

This will imply that in the usual Half Schlumberger were B is placed at a position three times $(AB/2)$:

$$3 \left(\frac{AB}{2} \right) = 2K_F$$

And for the Modified Half Schlumberger where B is placed at four times $\{4(AB/2)\}$:

$$4 \left(\frac{AB}{2} \right) = 2(AB) = xK_F \quad (18)$$

From (18) and (19), it implies:

$$x = \frac{8}{3} \quad (19)$$

So, equation (19) becomes:

$$K_{MH} = 2(AB) = xK_F = \frac{8}{3}K_F \quad (20)$$

Consequently;

$$\rho_a = \frac{8}{3}RK \quad (21)$$

Equation (22) is a modified equation from the existing equations of Full and Half Schlumberger and it can be used to compute the geometry factor for the Modified Half Schlumberger (see table 3).

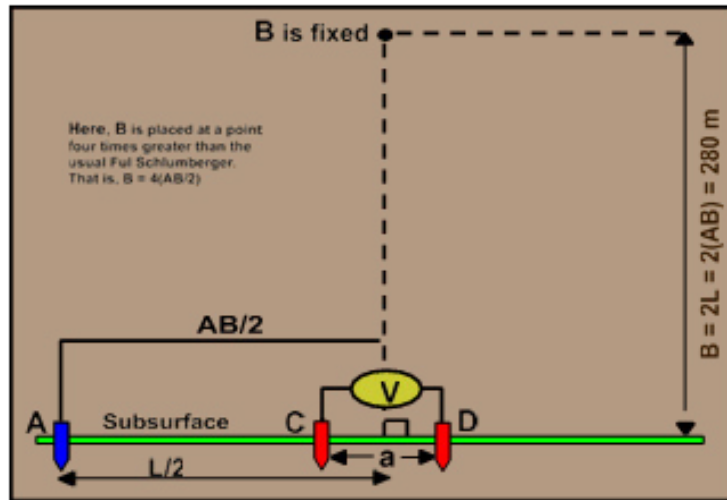


Figure 5: Configuration of the Modified Half Schlumberger Arrays (B at 2L)

Raw Data Obtained from a Crystalline Basement Complex Terrain

Tables 2 and 3 show the raw data acquired from a crystalline basement complex terrain using both arrays (SH and SMH) for VES 1. The resistivity (R) values are the direct values measured by the Ohmega resistivity meter, while AB and CD are measured

from the physical arrangement of the four (4) electrodes. Consequently, the K-factors for both arrays were calculated from equations (16) and (21), while the apparent resistivity values were computed from equations (17) and (22), for the two Schlumberger arrays and presented in tables 2 and 3.

Table 2: Geometry Factors and Computed Apparent Resistivity Values for Half Schlumberger Array

S/N	$\left(\frac{AB}{2}\right)$ (m)	$\left(\frac{CD}{2}\right)$ (m)	Geometry -factor $K_H = 2K_F$	Resistivity Values R (Ω)	Apparent Resistivity $\rho_a = K_H R$ (Ωm)
1	1.0	0.3	9.52	85.63	815.198
2	1.5	0.3	22.62	23.48	621.598
3	2.0	0.3	40.94	13.62	598.543
4	3.0	0.3	93.3	6.729	627.816
5	4.5	0.3	211.12	3.252	686.563
6	7.0	0.3	512.2	1.362	697.617
7	7.0	1.0	150.8	4.523	682.069
8	10.0	1.0	311.02	2.134	663.717
9	15.0	1.0	703.72	0.7898	555.798
10	20.0	1.0	1253.5	0.3395	425.563
11	30.0	1.0	2828.3	0.1484	419.720
12	45.0	1.0	6358.6	0.0786	499.786
13	45.0	5.0	1256.64	0.2714	341.052
14	70.0	5.0	3063.06	0.1863	570.648

Table 3: Geometry Factors and Computed Apparent Resistivity Values for the Modified Half Schlumberger Array

S/N	$\left(\frac{AB}{2}\right)$ (m)	$\left(\frac{CD}{2}\right)$ (m)	Geometry -factor $K_{MH} = \frac{8}{3}K_F$	Resistivity Values R (Ω)	Apparent Resistivity $\rho_a = K_{MH} R$ (Ωm)
1	1.0	0.3	12.6933	62.63	794.983
2	1.5	0.3	30.1600	21.48	647.837
3	2.0	0.3	54.5867	11.62	634.297
4	3.0	0.3	124.400	6.299	783.596
5	4.5	0.3	281.493	3.017	849.265

6	7.0	0.3	682.933	1.112	759.422
7	7.0	1.0	201.067	3.791	762.244
8	10.0	1.0	414.693	1.894	785.430
9	15.0	1.0	938.293	0.6997	656.524
10	20.0	1.0	1671.33	0.2953	493.545
11	30.0	1.0	3765.73	0.1105	416.114
12	45.0	1.0	8478.13	0.0697	590.926
13	45.0	5.0	1675.52	0.220	368.614
14	70.0	5.0	4084.08	0.1461	596.684

Data Processing and Interpretation

Data Processing

The data obtained in a crystalline basement complex terrain (Tables 2 and 3), were fed into the computer software as the initial raw data model parameter in a forward iterative modelling technique using RES 1D computer software (version 1.00.07 Beta) [7]. The interpreted results, which consist of the subsurface layers' resistivity values and their layer thicknesses) are presented in table 4. These results were further used for qualitative and comparative analysis for the Half Schlumberger and the Modified Half Schlumberger array. Before applying the complex computer software, we employ an excel Microsoft for a few rough work

ideas. The typical resistivity curves of VES 1 obtained from Res 1D for both arrays with a pair of resistivity curves for four layers are presented in Fig 6. The generated curves by Res 1D can be classified simply into four (4) basic curve shapes, (where we have A, H, K, and Q) which can be combined to describe more complex field curves that may have many layers [4]. This curve allows us to determine the model parameters like initial model layers and the curve types. Though, in this research, we have four generated curves (such as KH, QH, KHK, and AA). We, however, noted that the curve types generated from both arrays produced the same curves across all the VES stations.

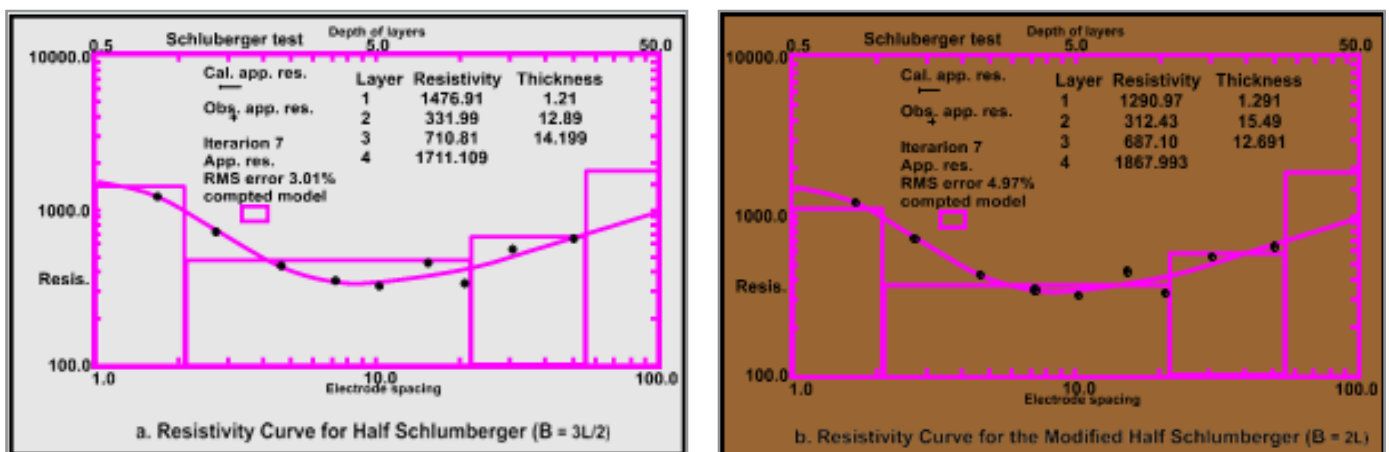


Figure 6: Typical Resistivity Curves of Schlumberger Arrays Configuration for VES 1

Interpreted Values

Table 4 shows the data interpreted from Res 1D, which gives us the subsurface layer's resistivities and its thickness for both arrays across all the VES points, while Table 5 shows the comparative analysis of the Half Schlumberger and the Modified Half Schlumberger. The results however show that both arrays are nearly the same at all points.

Table 4: Interpreted Results Showing the layer Resistivity and its Thickness across the Nine (9) VES Stations.

VES Pts	Geologic Layers	Half Schlumberger when B is placed at distance $B = 3(AB/2)$		Half Schlumberger when B is placed at distance $B = 4(AB/2)$	
		Apparent Resistivity ($\rho_a/\Omega m$) Layer's Thickness (h/m)	Overburden Thickness d/m	Apparent Resistivity ($\rho_a/\Omega m$) Layer's Thickness (h/m)	Overburden Thickness d/m
V1	1/2/3/4	1477/332/711/1711 1.2/12.9/14.2	28.3	1291/312/687/1868 1.3/15.5/12.7	29.5
V2	1/2/3/4	1999/682/49/1719 0.7/5.1/11.9	17.7	1879/682/62/2022 1.0/4.9/14.4	20.0

V3	1/2/3/4/5	179/85/212/50/14992 1.3/4.1/5.4/10	20.8	119/85/212/50/15119 1.5/5.3/3/15.7	22.5
V4	1/2/3/4	1901/617/88/49971 0.8/6.7/13.3	20.9	1717/499/77/48001 0.9/5.7/17.9	24.2
V5	1/2/3/4	1901/617/88/49971 0.8/6.7/13.3	21.0	177/41/101/9101 3.1/3.9/18.3	25.3
V6	1/2/3/4	171/333/611/1807 1.8/21.1/7.2	30.1	133/305/599/1907 2.1/22.4/7.9	32.4
V7	1/2/3/4	171/333/611/1807 1.8/21.1/7.2	21.3	133/305/599/1907 2.1/22.4/7.9	24.9
V8	1/2/3/4	179/322/509/20031 2.1/22/9.9	34.0	152/299/599/18009 2.3/23/10.2	35.8
V9	1/2/3/4	500/2401/142/3510 2.9/4.1/18.3	25.3	457/2111/133/4010 3.2/3.7/19.7	26.6

Results and Discussion

The results of the interpreted data for this research were presented in tables, line graphs and histogram graphs. The geo-electric/geologic model or depth section was defined based on the results of several geo-electric surveys [15, 44, 45], using ranges of resistivity values. After the quantitative interpretation, the results show the Half Schlumberger (SH), where $B = 3(AB/2) = 210$ m and the Modified Half Schlumberger (SMH), where $B = 2(AB) = 280$ m, are highly similar and are virtually the same for all VES points with about 94% in similarity as shown in table 5. This 94% similarity agreed with the previous research works with the percentage similarities of 97%, 98%, and 97% respectively [31, 33, 20]. The processed data presented in Figures 7, 8, 9 and 10, show that the Half Schlumberger and the modified Half Schlumberger are nearly the same at all VES stations. This infinitesimal variation indicates that the Half Schlumberger and the modified Half Schlumberger are effective and reliable, which can be adopted for any Vertical Electrical Sounding geophysical survey where the traditional (Full) Schlumberger is effective, reliable, and applicable as well. However, with the emphasis on the Modified Half Schlumberger array, it was observed that the SMH gives a higher topsoil thickness with about 0.27 m compared to SH, but the reverse is the case for topsoil resistivity,

as the SH is seen to have higher resistivity values as seen in table 5. Though, the variation in topsoil resistivity is almost inconsequential, having 96% similarity. Interestingly, the SMH provides a higher aquifer thickness with an extension of 2.0 m thickness. This suggests that the SHM probes deeper than the usual SH. The average aquifer resistivity value was found to be 225 Ω m and 228 Ω m for the SH and SHM respectively. This variation in aquifer resistivity is high infinitesimal and considered insignificant, having 99% similarity.

A study shows that the basic need of human beings is water and it should be considered a priority, the major emphasis of the SHM is on the overburden thickness which enhances the groundwater potential [26]. From Table 5, it was noted that; while the SH produced 24.4 m overburden thickness, the SMH attained 26.8 m overburden thickness. This high variation in overburden thickness (2.4 m) makes the SHM unique, better, and preferable technique for groundwater exploration especially in a highly congested environment. From the last layer resistivity, there were no significant changes observed between both arrays having noted high resistivity values (12,000 Ω m) for arrays, we concluded that; the last layer is fresh basement rocks.

Table 5: Geoelectric Parameters of The Study Area Showing the Correlation in Percentage for Both Arrays

SN	Lithologs of the geoelectric section	Half Schlumberger when B is at $L = 3(AB/2) = 300$ m	Modified Half Schlumberger when B is at $L = 2(AB) = 400$ m	Similarity in percentage
1	Topsoil Thickness	1.70 m	1.97 m	86 %
2	Topsoil Resistivity	796 Ω m	791 Ω m	96 %
3	Aquifer Thickness	20.0 m	22 m	91 %
4	Aquifer Resistivity	225 Ω m	228 Ω	99 %
5	Overburden Thickness	24.4 m	26.8 m	91 %
6	Bedrock Resistivity	12910 Ω m	12771 Ω m	94 %
	Average			94 %

Fig 7 is the topsoil resistivity with an interesting resistivity value. The figure reveals that the modified half Schlumberger produced a topsoil resistivity that is infinitesimally low when compared to the usual Half Schlumberger at all VES stations. One major interesting thing about the resistivity values displayed in Fig 7, is the trend of variations. Considering Fig 7, it was discovered that the SMH

produced resistivity values that are less than that of SH across all the VES stations. That is, it can be concluded that the topsoil resistivity values for Half Schlumberger (SH), are always greater than that of the Modified Half Schlumberger (SMH), having observed these variations in all the nine (9) VES stations. Thus:

$$S_H > S_{MH} \quad (\text{in topsoil resistivity}) \quad (23)$$

The result in equation (23), is not strange because, the Schlumberger array at the near-surface effects generally varies much less, provided that only the current electrodes (AB) are moved, and this is why the Schlumberger array is often preferred for depth sounding [14]. However, the topsoil thickness plotted in Fig 8 seems to take a different direction as the topsoil thickness varies in the opposite direction. In Fig 8, the SH and the SMH

are nearly the same, though, SMH seems to have higher topsoil thickness in all locations, and this is not unconnected to the fact the SHM probes deeper than SH. That is, we can also conclude that the SH array is always less than that of SMH in terms of topsoil thickness, since the disparities occur at all the VES stations. Thus, we say:

$$S_H > S_{MH} \quad (\text{in topsoil Thickness}) \quad (24)$$

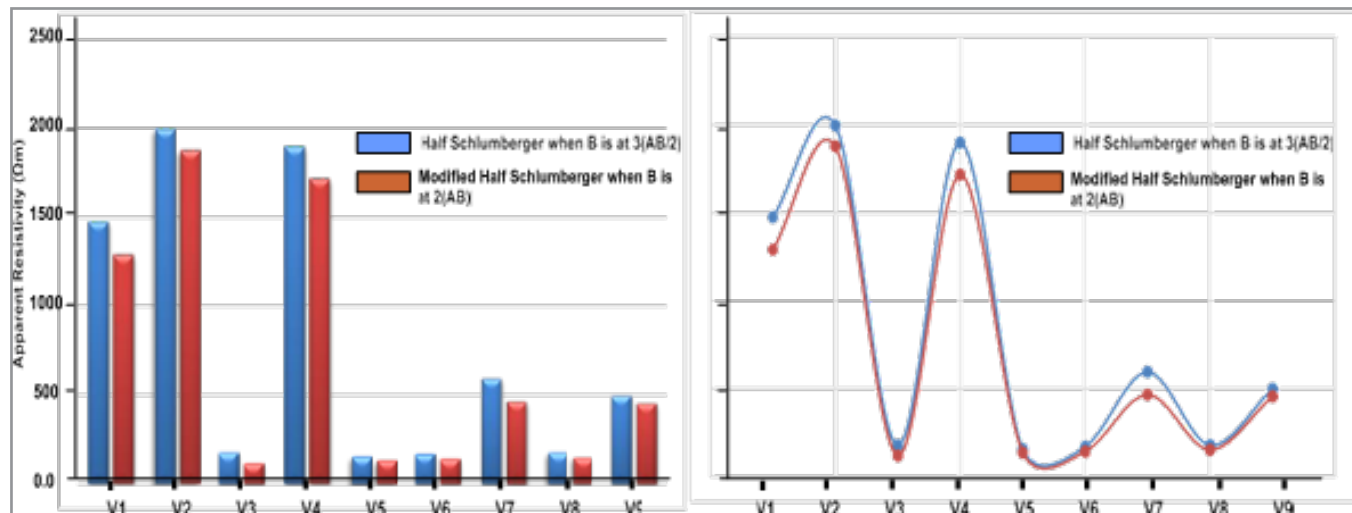


Figure 7: The bar Chart Graph of the Topsoil Resistivity of the Study Area

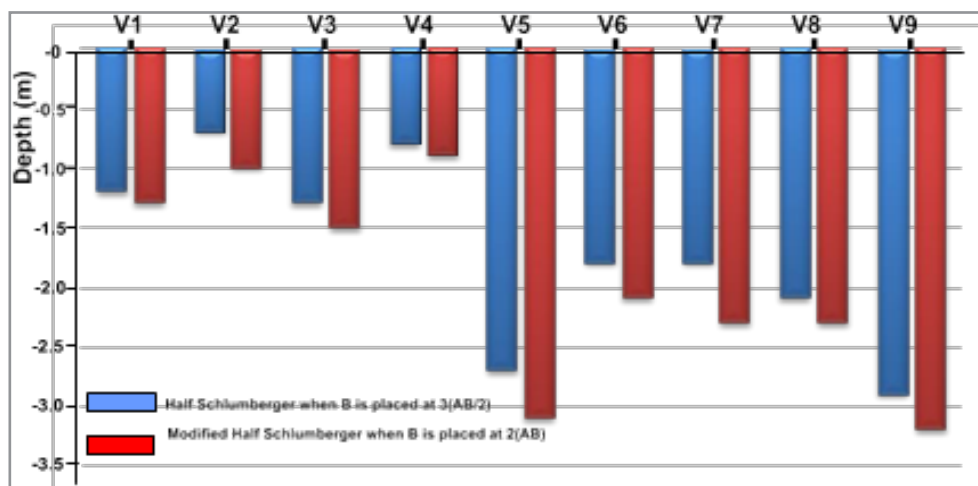


Figure 8: The bar Chart Graph of the Topsoil Thickness of the Study Area

Figures 9 and 10, show the basement resistivity and the overburden thickness respectively. In Fig 9, the modified half Schlumberger indicates an infinitesimally high basement resistivity compare to the usual Half Schlumberger in almost all the locations, except in location V8. The variation in V8 may not be unconnected with the fact that the modified half Schlumberger probes deeper than the usual half Schlumberger, thereby causing the current to hit the basement rocks at a more fresh and harder depth, where there is no element of weathering and fracturing activities. On the other hand, the modified half Schlumberger shows an interesting value in Fig 10, being the overall (overburden) thickness of the subsurface terrains. Though, the over-

burden thickness values are nearly the same at all VES points, but, the Modified Half Schlumberger probe is deeper when compared with the usual Half Schlumberger, with an extension of 2.4 m (240 cm). This implies that the Modified Half Schlumberger is relatively more effective than the usual Half Schlumberger, in a deeper subsurface investigation. Therefore, we can technically say, the overburden thickness of the half and the modified half Schlumberger arrays are related as follow:

$$S_H < S_{MH} \quad (\text{in terms of overburden thickness}) \quad (25)$$

Equation (25) is directly opposite of equation (23). That is, it can be concluded that the Half Schlumberger and Modified Half Schlumberger arrays are highly reliable and effective. Therefore, S_{MH} is recommended for any Vertical Electrical Sounding geo-

physical survey where the traditional full Schlumberger survey is applicable, especially in a congested and built environment, where deeper subsurface information is required and the space available is highly limited.

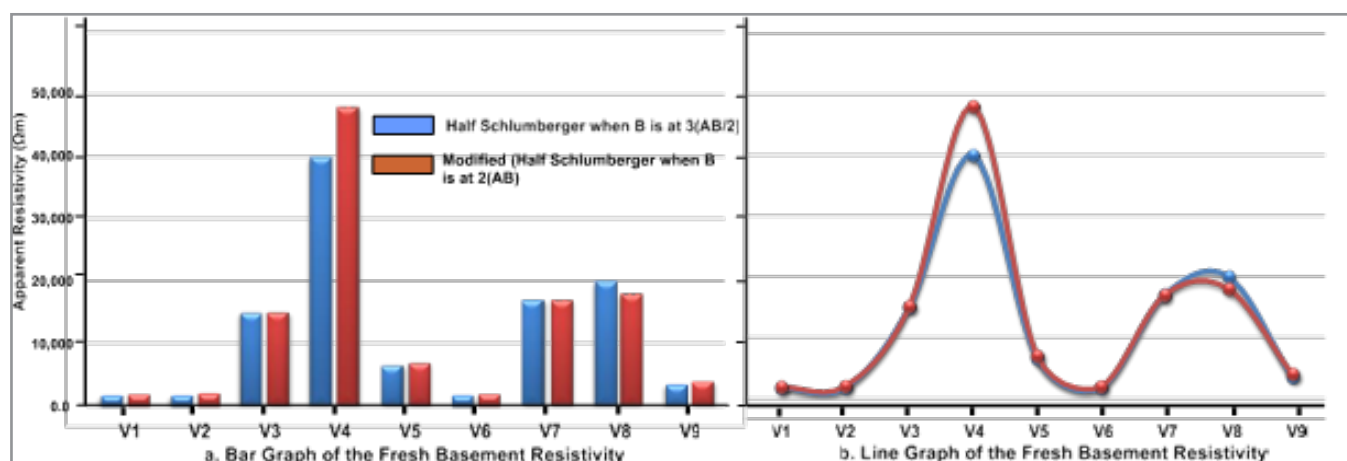


Figure 9: The bar Chart Graph of the Fresh Basement Resistivity of the Study Area

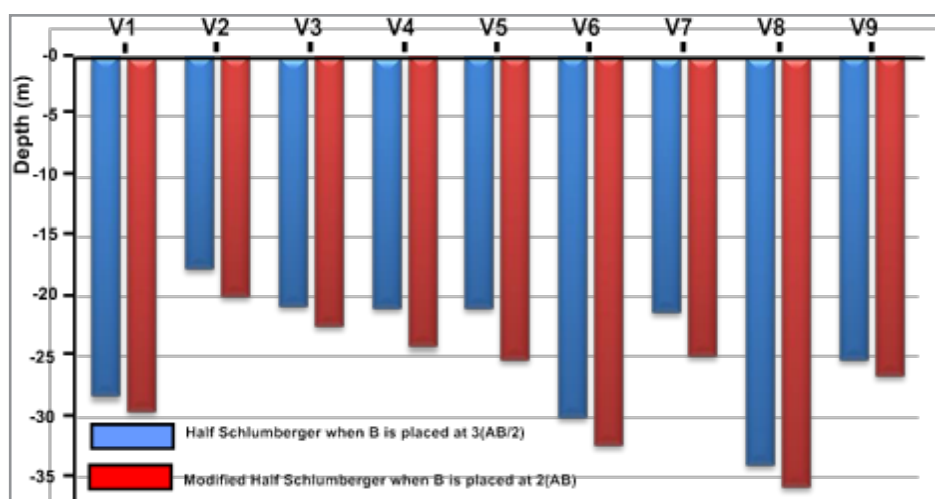


Figure 10: The bar chart Graph of the Overburden Thickness of the Study Area

Comparison of the Usual Half Schlumberger and the Modified Half Schlumberger

The traditional SM array has a moderate depth of investigation and strong signal strength which is inversely proportional to its geometric factor which is used in calculating the apparent resistivity. The SMH has a high depth of investigation with high signal strength and is preferred in a deep subsurface investigation. This implies that; the SMH is the most sensitive configuration to vertical variations. However, both arrays are not suitable for investigations in a noisy site because of their high signal strength. Also, they are less sensitive to horizontal variations coverage with increased electrode spacing and 3D structures. On the other hand, the choice of the array for site investigation is usually influenced by the depth of investigation and environmental factors. While the environmental factor is defined by available space, the depth of investigation factor is defined by deeper subsurface information or depth penetration required. That is; the SMH is considered the best array, in a congested environment where deeper subsurface information is required.

Conclusion and Recommendations

In Schlumberger array configurations, it was noted that it is almost impossible or extremely difficult to operate; since the spread to depth, the ratio is 2:1. This implies that; it is extremely difficult or impossible to probe beyond the depth of 100 m. The interpretation is not ambiguous because the software can take care of the errors for matching with the standard curves. In doing this, the original of the layers may change and the interpretation may differ depending upon the handler. The Schlumberger technique is fast and easy, but the SH and the SMH are faster and easier to operate; because it is less time consuming, require less manpower and are not limited in a congested environment. The task of interpreting data is an easy job by the curve matching technique. It is time-consuming to identify different curves, especially when considering a terrain with more layers. Though, it was observed that; while the Full Schlumberger or other electrical methods like Wenner cannot be applied in a region where there is urban development for their lateral spread of the electrodes, the SH and the SMH arrays are not limited in a congest-

ed environment because only one moving electrode is required. Based on the geo-electrical data interpretation, it was noted that both SH and the SMH arrays show posit match in terms of all the subsurface parameters obtained across all the VES. The results of the interpreted data show that the SH and SMH are highly correlated (about 94% in similarity. For instance, $SH > SMH$, in topsoil resistivity and thickness across all the nine (9) VES stations. The modified equation ($\rho_a = \frac{8}{3}RK$), was used to calculate the K-factor for the Modified Half Schlumberger and the result shows that the geometry (K) factor for SMH is valid, efficiency, and reliable. Based on the analysis, the SMH array is a practicable alternative array to the usual full Schlumberger and the Half Schlumberger array for any geophysical exploration, especially in a region where the aquifer is deep with limited space. Due to the ability of SMH to relatively probe deeper, it is considered reliable and more effective in delineating groundwater potential especially when deeper subsurface information is required and the available space is highly limited. In addition, the main strength of SMH is its ability to relatively probe deeper, which may lead to the reduction of the signal to noise ratio.

Declaration of Conflict Interest

In compliance, I hereby declare that there is no conflict of interest in this research work. All information provided in this work has been duly acknowledged in the text and the references provided. No part of the work has been previously published in any journal.

References

1. Caers, J., Scheidt, C., Yin, Z., Wang, L., Mukerji, T., et al. (2022). Efficacy of information in mineral exploration drilling. *Natural Resources Research*, 31, 1157-1173.
2. Alao, J. O., Lawal, K. M., Dewu, B., & Raimi, J. (2023). The evolving roles of geophysical test sites in engineering, science, and technology. *Acta Geophysica*.
3. Omeiza, A. J., Lawal, K. M., Dewu, B., & Raimi, J. (2023). Development of geophysical test sites and its impacts on the research and education activities. *Bulletin of Engineering Geology and Environment*, 82.
4. Telford, W. M., Geldart, L. P., & Sheriff, E. E. (1990). *Applied geophysics* (2nd ed.). Cambridge University Press.
5. Akintorinwa, O. J., & Abiola, O. (2012). Comparison of Schlumberger and modified Schlumberger arrays VES interpretation results. *Research Journal in Engineering and Applied Sciences*, 1, 190-196.
6. Froyland, G., Menabde, M., Stone, P., & Hodson, D. (n.d.). The value of additional drilling to open-pit mining projects. In R. Dimitrakopoulos (Ed.), *Advances in Applied Strategic Mine Planning* (pp. 120-137). Springer Cham.
7. Loke, M. H. (2000). *Electrical imaging surveys for environmental and engineering studies: A practical guide to 2-D and 3-D surveys* (6).
8. Alao, J. O. (2023). Impacts of open dumpsite leachates on soil and groundwater quality. *Groundwater for Sustainable Development*, 20, 100877.
9. Alao, J. O., Fahad, A., Abdo, G. H., Ayejoto, D. A., Almohamad, H., et al. (2023). Effects of dumpsite leachate plumes on surface and groundwater and the possible public health risks. *Science of The Total Environment*, 897, 165469.
10. Alao, J. O., Lawal, H. A., & Nur, M. (2023). Investigation of groundwater vulnerability to open dumpsites and its potential risk using electrical resistivity and water analysis. *Heliyon*, 8, 13265.
11. Hermawan, O. R., & Putra, D. P. E. (2016). The effectiveness of Wenner-Schlumberger and dipole-dipole array of 2D geoelectrical survey to detect the occurrence of groundwater in the Gunung Kidul karst aquifer system, Yogyakarta, Indonesia. *Journal of Applied Geology*, 1, 71-81.
12. Alao, J. O., Yusuf, M. A., Nur, M. S., Nuruddeen, A. M., & Ahmad, M. S. (2023). Delineation of aquifer promising zones and protective capacity for regional groundwater development and sustainability. *SN Applied Sciences*, 5, 149.
13. Alao, J. O., Fahad, A., Danladi, E., Danjuma, T. T., Mary, E. T., & Diya'ulhaq, A. (2023). Geophysical and hydrochemical assessment of the risk posed by open dumpsite at Kaduna Central Market, Nigeria. *Sustainable Water Resources Management*, 9(5), 170.
14. John, M. (2003). *Field geophysics* (3rd ed.). John Wiley & Sons Ltd.
15. Adebisi, N. O., & Oloruntola, M. O. (2006). Geophysical and geotechnical evaluation of foundation conditions of a site in Ago-Iwoye area, southwestern Nigeria. *Journal of Mining and Geology*, 42, 79-84.
16. Aweto, K. (2012). Aquifer vulnerability assessment at Oke-Ila area, southwestern Nigeria. *International Journal of Physical Sciences*, 6, 7574-7583.
17. Dogara, M. D., & Alao, J. O. (2017). Exploration for gypsum using electrical resistivity method at Ikpeshi, Edo State, Nigeria. *KADA Journal of Physics*, 1, 67-77.
18. Dogara, M. D., & Alao, J. O. (2017). Preliminary estimate of gypsum deposit based on Wenner and Schlumberger electrical resistivity methods at Ikpeshi, Edo State, Nigeria. *Science World Journal*, 12, 1597-6343.
19. Dogara, M. D., Aboh, H. O., Alao, J. O., & Kogi, K. A. (2017). The aquifer overlying the basement complex in some parts of Dan-Hono, Kaduna, Nigeria. *KADA Journal*, 2, 45-52.
20. Alao, J. O., Dogara, M. D., Danlami, A., & Samson, E. E. (2019). Comparative assessment of half Schlumberger configuration as an alternative method to the conventional Schlumberger configuration at Trade Centre, Mani-Nissi Village, Kaduna, Nigeria. *SSRG International Journal of Applied Physics (SSRG-IJAP)*, 6, 51-56.
21. Aboh, H. O., Dogara, M. D., & Alao, J. O. (2016). Evaluation of the geotechnical parameters in part of Kaduna, Kaduna State, Nigeria. *World Journal of Applied Science and Technology*, 8, 108-117.
22. Omeiza, J. A., Abdulwahab, O. O., Nur, M. S., Danjuma, T. T., Emmanuel, J., et al. (2022). Effect of an active open dumpsite on the Earth's subsurface and groundwater resource. *Asian Journal of Physical and Chemical Sciences*, 10, 15-24.
23. Alao, J. O., Danjuma, T. T., Nur, M. S. (2022). Electrical conductivity for selection of viable land for agricultural activities and suitable sites for borehole. *Asian Journal of Geological Research*, 5, 37-50.
24. Alao, J. O., Danjuma, T. T., Ahmad, M. S., & Diya'ulhaq, A. (2022). Application of geoelectric resistivity technique to a selected site for agricultural practices at Kujama farmland, Kaduna, Nigeria. *SSRG International Journal of Geoinformatics and Geological Science*, 9, 46-51.
25. Alao, J. O., Ahmad, M. S., Danjuma, T. T., Ango, A., & Emmanuel, J. (2022). Assessment of aquifer protective capac-

- ity against surface contamination: A case study of Kaduna Industrial Village, Nigeria. *Physical Science International Journal*, 26, 43-51.
26. Vasantrao, B. M., Bhaskarrao, P. J., Mukund, B. A., Baburao, G. R., & Narayan, P. S. (2017). Comparative study of Wenner and Schlumberger electrical resistivity method for groundwater investigation: A case study from Dhule district (M.S.), India. *Applied Water Science*, 7, 4321-4340.
 27. Veronica, P., Stefano, M., & Riccardo, F. (2019). A review of the advantages and limitations of geophysical investigations in landslide studies. *International Journal of Geophysics*, 1-27.
 28. Dena, O. S., Obeso, O. G., Doser, C. D., Leyva, J., Rascon, E., et al. (2012). Using subsurface geophysical methods in flood control: A resistivity survey to define underground storage capacity of a sand body in Ciudad Juárez, Mexico. *Geofísica Internacional*, 51, 225-249.
 29. Okpoli, C. C. (2013). Sensitivity and resolution capacity of electrode configurations. *International Journal of Geophysics*, 1-12.
 30. Moreira, C. A., Lapola, M. M., & Carrara, A. (2016). Comparative analyses among electrical resistivity tomography arrays in the characterization of flow structure in free aquifer. *Geofísica Internacional*, 55, 119-129.
 31. Anjorin, M. P., & Olorunfemi, M. O. (2011). A short note on comparative study of Schlumberger and half Schlumberger arrays in vertical electrical sounding in a basement complex terrain of Southwest Nigeria. *The Pacific Journal of Science and Technology*, 528-533.
 32. Nick, B., & Katerina, K. (2011). Application of half Schlumberger configuration for detecting karstic cavities and voids for a wind farm site in Greece. *Journal of Earth Sciences and Geotechnical Engineering*, 1, 101-116.
 33. Oladunjoye, M., & Jekayinfa, S. (2015). Efficacy of Hummel (Modified Schlumberger) arrays of vertical electrical sounding in groundwater exploration: Case study of parts of Ibadan Metropolis, Southwestern Nigeria. *International Journal of Geophysics*, 2, 1-24.
 34. Kure, N., Aboh, H. O., Jimoh, R., Alao, J. O., & Isaac, H. D. (2019). The delineation of the aquifer overlying the basement complex within Ahmadu Bello University (Main Campus) Zaria. *British Journal of Applied Sciences*, 19, 1-9.
 35. Keller, G. V., & Frischknecht, F. C. (1979). *Electrical methods in geophysical prospecting*. Peramon Press.
 36. Kearey, P., Brooks, M., & Hill, I. (2002). *An introduction to geophysical exploration* (3rd ed.).
 37. Abdullahi, N., & Udensi, E. E. (2008). Vertical electrical sounding applied to hydrogeologic and engineering investigations: A case study of Kaduna Polytechnic Staff Quarters, Nigeria. *Nigeria Journal of Physics*, 20, 175-188.
 38. Bayowa, O. G., & Olayiwola, N. S. (2015). Electrical resistivity investigation for topsoil thickness, competence, and corrosivity evaluation: A case study from Ladoke Akintola. *International Conference on Geological and Civil Engineering*, 80, 52-56.
 39. Omeiza, J. A., & Dary, M. D. (2018). Aquifer vulnerability to surface contamination: A case of the new millennium city, Kaduna, Kaduna State Nigeria. *World Journal of Applied Physics*, 3, 1-12.
 40. Nur, M. S., Aniedi, J. B., Udo, A., Dawaki, T. M., & Alao, J. O. (2022). Investigation of groundwater of Pindiga Town, Akko Local Government Area of Gombe State, using vertical electrical sounding (VES). *AFIT Journal of Science and Engineering Research*, 2, 153-167.
 41. John, M. (1997). *An introduction to applied and environmental geophysics*. John Wiley & Sons.
 42. El-Arabi, H. S. (2008). *Electrical prospective methods*. Suez Canal University, Faculty of Science, Department of Geology.
 43. Fadele, S. I., Jatua, S. B., & Patrick, N. O. (2012). Geophysical engineering investigation around Makiyaye village, Shika area within the basement complex of North-Western Nigeria. *International Journal of Engineering Research and Applications*, 1, 1143-1153.
 44. Dogara, M. D., Alao, J., Abdullahi, H., Ezekiel, J., & George, J. (2017). Delineation of the geotechnical parameters within the Kaduna Refining and Petrochemical Corporation layout. *World Journal of Applied Physics*, 2, 36-42.
 45. Abdullahi, D., Omeiza, A. J., Narimi, A. M., Musa, S., & Nagoda, N. M. (2022). Assessing the water content and electrical conductivity of soil samples for agricultural precision using a digital dialysate meter. *1st Faculty of Science International Conference FSIC*, 134-140.